MICRO-SEISMOMETERS VIA ADVANCED MESO-SCALE FABRICATION

Caesar T. Garcia, Guclu Onaran, Brad Avenson, Matthew Ellis, and Neal A. Hall

Silicon Audio, LLC

Sponsored by the National Nuclear Security Administration

Contract No DE-FG02-08ER85106

ABSTRACT

The Department of Energy (DOE) and the National Nuclear Security Administration (NNSA) seek revolutionary innovations with respect to miniature seismic sensors for the monitoring of nuclear detonations. Specifically, the performance specifications are to be consistent with those obtainable by only an elite few products available today, but with orders of magnitude reduction in size, weight, power, and cost. The proposed commercial innovation calls upon several advanced fabrication methods and read-out technologies being pioneered by Silicon Audio, including the combination of silicon microfabrication, advanced meso-scale fabrication and assembly, and the use of advanced photonics-based displacement / motion detection methods. In Phase 1, the development team demonstrated the feasibility of the proposed innovation with a "macro" prototype. Specifically, two major goals were met: 1) proof mass elements capable of achieving sub 1ng noise were demonstrated, and 2) the high-fidelity, ultra-miniature motion detection principle used to monitor proof mass vibrations was successfully demonstrated. The upcoming Phase II development will focus on innovations aimed at complete sensor implementation. These include addressing low frequency noise challenges, low power consumption, ultra-miniature size, and low cross axis sensitivity. Successful implementation will result in a demonstration unit roughly the size of a 9-volt battery and with the ability to address advanced national security needs of the DOE/NNSA. Additional applications envisioned include military/ defense, scientific instrumentation, oil and gas exploration, inertial navigation, and civil infrastructure monitoring.

OBJECTIVES

The DOE/NNSA seeks revolutionary innovations with respect to miniature seismic sensors for the monitoring of nuclear detonations. Specifically, the performance specifications are to be consistent with those obtainable only by a few elite products available today, but with orders of magnitude reduction in size, weight, power, and cost. The specific sensor specifications solicited are as follows:

- Size – less than 1 in^3
- Power – less than 100 mW
- Sensor self noise – below USGS NLNM, or approximately 0.5 ng/√Hz
- Dynamic range at least 120 dB over a frequency band of 0.2 to 40 Hz.

In a prior review (Hall, 2008), we summarized basic design considerations for any proposed technology aiming to meet the aforementioned specifications. In particular, it was shown that meeting the noise requirement demands both a) ultra-low thermal mechanical noise from the seismometer proof mass, and b) high resolution displacement measuring capability of the proof mass motion. As an example, a design with a 2 gram proof mass and 50 Hz open loop resonant frequency may be considered. In this case, achieving the required 0.5 ng/√Hz acceleration noise requires a resonance quality factor Q of 100 and an ultra-low displacement resolving capability of 50 fm/√Hz (Hall, 2008). The high resonance Q, in-turn, requires the use of closed-loop feedback altered dynamics to realize the desired flat frequency response of the sensor. This discussion provides the motivation for Silicon Audio's proposed design innovation, which calls upon advanced meso-scale fabrication of mechanical proof-mass elements, photonics-based displacement / motion detection, micro-scale optoelectronic integration, and the integration of closed-loop sensing modalities for high stability and high dynamic range. In subsequent sections, Phase I results are presented which demonstrate the feasibility of the proposed approach. The figure below summarizes Phase I measurement results and Phase II projections plotted against the earth's background noise and the current best micro-electromechanical system (MEMS) demonstrations.

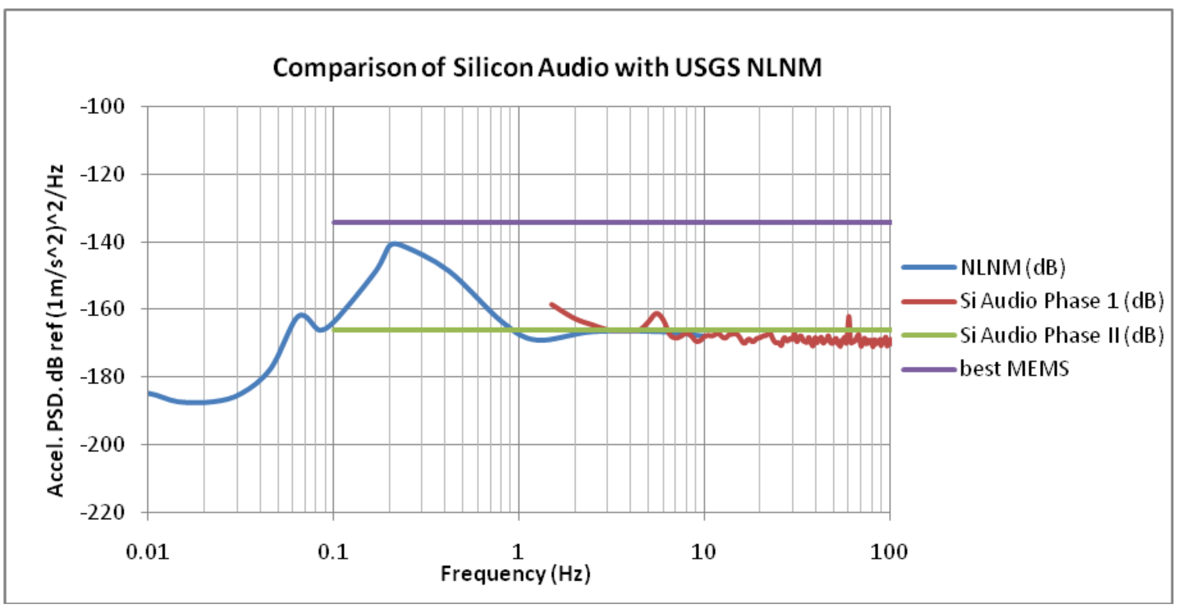

Figure 1. Acceleration noise power spectral density of the earth's background noise (NLNM), current best MEMS demonstrations, and Silicon Audio's Phase I and projected Phase II results.

Proposed Sensor Innovation

The sensor innovation must incorporate a proof mass displacement detection method capable of resolving 50 fm/√Hz. A major component of this innovation is the integration of an advanced photonics-based readout architecture with meso-scale (i.e., larger than MEMS) mechanical proof mass structures. The focus of this review article is on one of the motion detection principles being investigated, which is illustrated in the following figure.

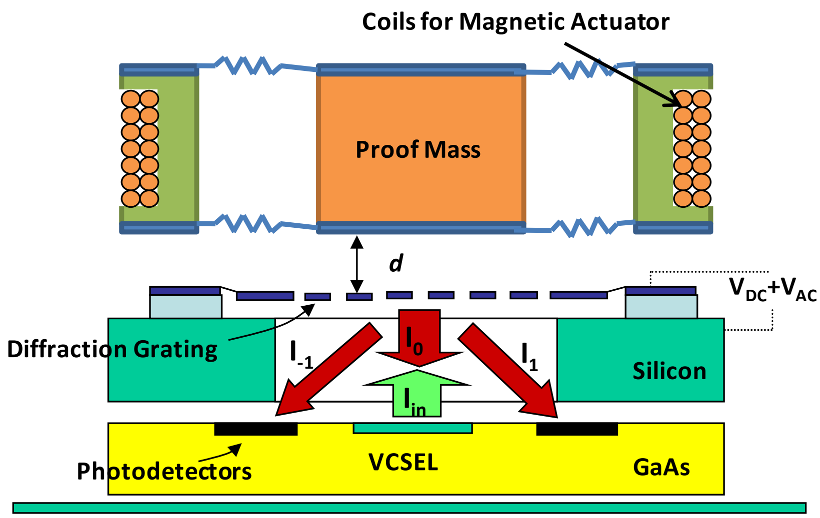

Figure 2. Schematic of a photonics based motion detection principle being developed by Silicon Audio. Light from a semiconductor laser such as a vertical cavity surface emitting laser (VCSEL) illuminates a diffraction grating fabricated on silicon. A portion of the incident light reflects directly off of the grating fingers, while the remaining light travels in between the grating fingers and to the proof mass and back to accrue additional phase. A diffracted field results consisting of a zero and higher orders whose angles remain fixed, but whose intensities are modulated by the relative distance between the proof mass and grating with the sensitivity of a Michelson type interferometer.

A sensing method very similar to that summarized in the caption of Figure 2 has been demonstrated and described in detail in prior developments (Lee et al., 2004; Hall et al., 2007; Hall, et al., 2008). The diffraction grating in this system serves the function of an optical beamsplitter, directly reflecting half of the incident light while passing the remaining half to travel to the proof-mass and back to accrue additional phase. Being an optical interference based approach, the displacement resolving capability of the method is of very high fidelity – on the order of 20 fm/√Hz when using small 500μW semiconductor lasers. The intrinsic open loop dynamic range of this approach (i.e., clip level) is limited to approximately λ/4, where λ is the optical wavelength. This corresponds to the peak-to-trough range of an interference cycle (i.e. fringe cycle) and is approximately 212 nm for an 850 nm wavelength semiconductor laser. Considering that 20 fm displacement can be resolved over a 1 Hz bandwidth, the intrinsic dynamic range is then 140 dB. Over the 40 Hz measurement bandwidth of interest, the open-loop dynamic range is 124 dB.

It should be emphasized that the schematic in Figure 2 is not drawn to scale. The total dimensions occupied by the silicon and GaAs chips is approximately 1mm^3, whereas the meso-fabricated proof mass is approximately 1 cm x 1 cm x 0.5 cm. To emphasize this, a micrograph of a packaged VCSEL and 2-element discrete photodiode array is provided in Figure 3 along with a separate micrograph of a fabricated grating structure.

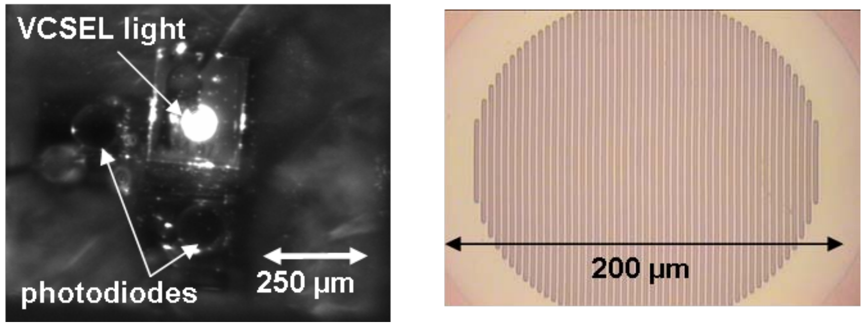

Figure 3. Left – micrograph of a packaged VCSEL (shown lasing) and centered amongst 2 photodiode elements. Right – micrograph of a fabricated grating structure. This structure has been etched into a 0.8µm thick silicon nitride layer.

The nominal distance "*d*" between the proof mass and grating structure as labeled in Figure 2 is relatively insignificant. It is important, however, that the interferometer be operated at a point of quadrature (i.e., a point of maximum slope and linearity on the interference curve). Figure 4 helps to clarify this by summarizing the theoretically predicted relationship between light intensity of the diffracted beams labeled in Figure 2 vs. the gap distance "d" also labeled in Figure 2. The center beam modulation is complementary to the sum of the exterior beams. Therefore, one can use the difference signal (in practice this is done by simple photocurrent subtraction), as the seismometer output signal. The linear operating region is highlighted in the figure. The slope of this curve is the displacement sensitivity of the detection method (after amplification through a photocurrent-to-voltage amplifier, the unit of the y axis is volts, and the sensitivity is therefore expressed in V/m).

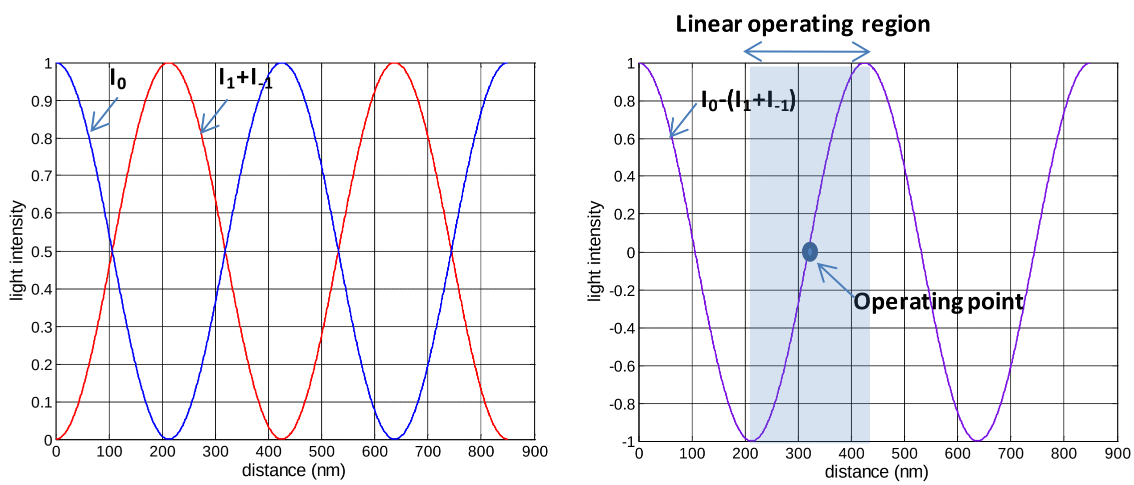

Figure 4. (left) Theoretically predicted relationship between the diffracted beams labeled in Figure 2 vs. gap distance "d" labeled in Figure 2. (right) The seismometer uses the difference signal to detect the proof mass motion within a single interference fringe.

Operation about a point of quadrature (i.e., the operating point labeled in Figure 4) can always be maintained by electrostatic actuation of the grating element as highlighted in Figure 2 with the applied electrostatic signals and/or by direct actuation of the proof mass using magnetic actuation. In addition, dynamic actuation of the proof mass also enables closed-loop measurement modalities. Closed loop operation is critical in high performance accelerometers, as the high *Q* of the open loop system required for low thermal noise must be electronically compensated for via feedback-altered-dynamics to achieve the desired flat frequency response (Liu and Kenny, 2001).

RESEARCH ACCOMPLISHED

The phase I feasibility study encompassed three primary goals:

1) Design, build, and experimentally demonstrate a meso-scale proof mass with a thermal mechanical noise level lower than 0.5ng/√Hz.
2) Demonstrate closed loop operation of the grating based motion detection system (summarized in Figure 2) and in particular the ability to use feedback to compensate for the high open loop resonance *Q* of the system, thereby demonstrating the desired flat frequency response.
3) Experimentally demonstrate the grating based motion detection system's ability to resolve the required 50fm/√Hz displacement.

The remainder of this review article will summarize accomplishments related to items 2 and 3.

Experimental Demonstration of Optical Interference

As a first experiment, the optical interference principle underlying the device operation was verified. This was accomplished by magnetically actuating the proof mass across a distance "d" relative the grating while measuring and recording the photodiode signals. The goal of this experiment is therefore to experimentally produce the theoretical curves presented in Figure 4. Figure 5 presents the result of this experiment, where the behavior predicted in Figure 4 is clearly verified. Note that the subtracted signal is the signal to be derived as the seismometer output. In operation, the proof mass is positioned to a point of maximum sensitivity (for example, d=2400nm in Figure 5), and small signal vibrations of the proof mass about this operating point are recorded.

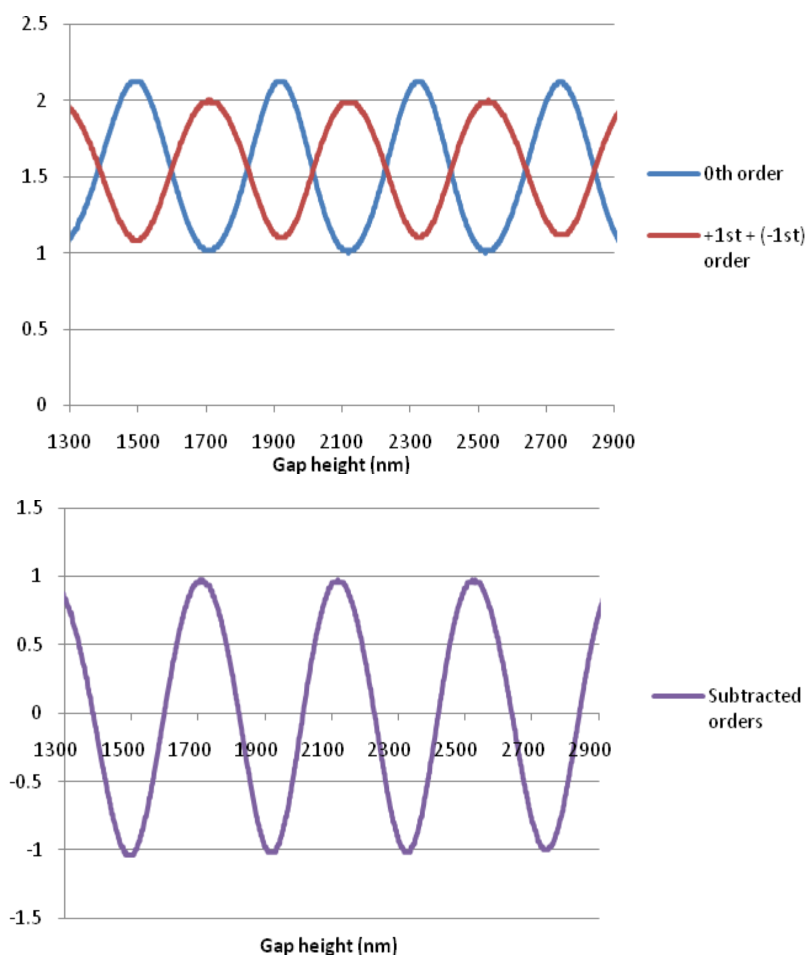

Figure 5. Experimental demonstration of the theoretical behavior predicted in Figure 4.

Experimental Demonstration of Closed Loop System Dynamics

A closed loop system schematic implemented in Phase I is depicted in Figure 6. Starting with an external inertial force input, the first block (i.e., the proof mass) converts this force into a displacement. The transfer function shown in this block is that of the well-known 2nd order system. The displacement is then converted into a voltage signal. The sensitivity noted in this block K_{tia} is simply the slope of the curve in Figure 4 (right) evaluated about the operating point. This measured displacement is the sensor output, V_{out}. The closed loop control block then applies magnetic forces to the proof mass in order to produce the desired flat frequency response. This technique has been used in other high fidelity measurement systems (Liu and Kenny, 2001).

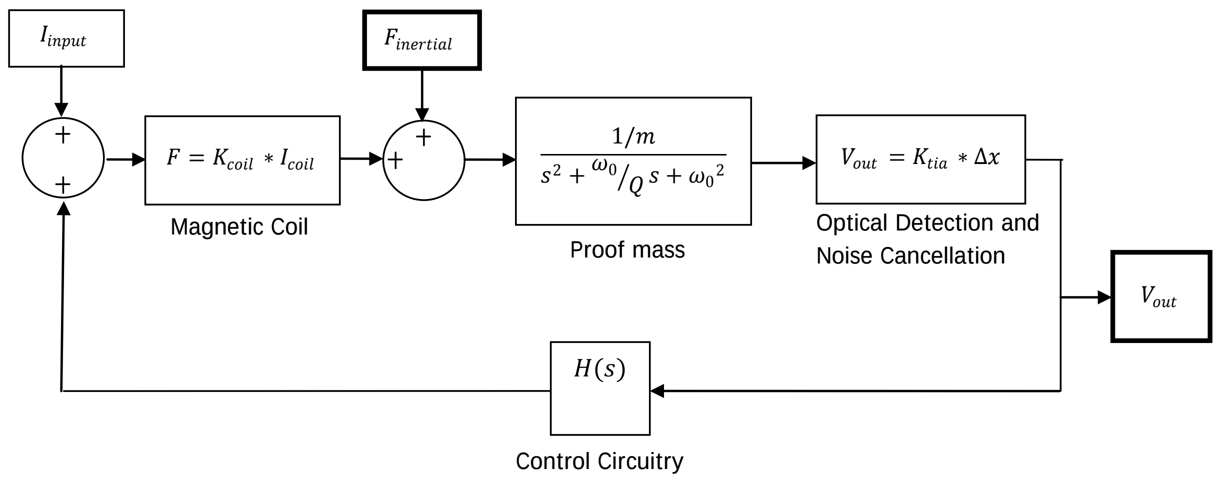

K_{coil} : Magnetic Coil force constant , units N/A
I_{coil} : Coil Current
I_{input} : Excitation current for response characterization
M, ω0 , Q : Open loop proof mass parameters
K_{tia} = TIA sensitivity V/m .
Δx = displacement relative to equilibrium position

Figure 6. Feedback control system schematic

A model for the closed loop system was developed in Matlab and utilized to design the control block. The additional coil current input shown in Figure 6 is used for self-test or dynamic characterization purposes. This port enables the generation of well controlled force inputs. The dynamics of the closed loop system were measured with a dynamic signal analyzer (model SRS 785) by applying a broadband swept sine input to this port while measuring the output signal. This experiment was repeated for several control settings to illustrate closed loop operation.

The results of this experiment are shown in Figure 7. The system can be modified with feedback forces to achieve the desired flat frequency response as shown by the "Measured response 3" case labeled in the figure. The frequency response below 1 Hz was filtered for convenience in these experiments, as the focus was on the resonance *Q*. The mechanical response of the proof mass below 1Hz is expected to be flat. Both stable operation and closed loop operation are successfully demonstrated with the sensor innovation summarized in Figure 2.

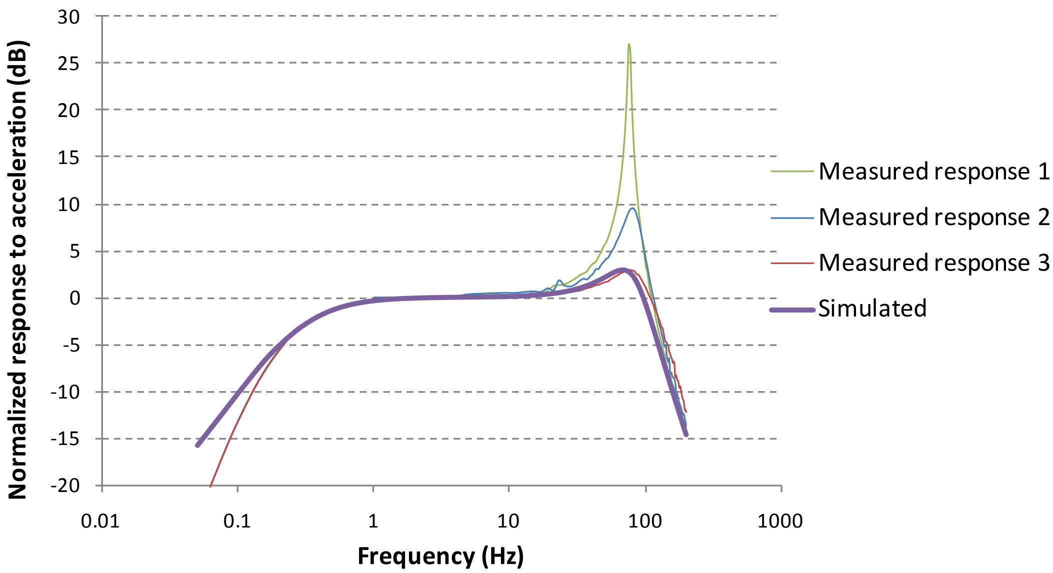

Figure 7. Measured closed loop system dynamics of the Phase I prototype. The low frequency roll-off is a design parameter and can easily be set to 100 mHz for the Phase II embodiment.

Displacement Noise Measurements

The third and final Phase I goal is demonstration of high fidelity displacement detection. For this experiment, the voltage noise spectrum at the sensor output is measured using the SRS 785 dynamic signal analyzer and referred to displacement units using K_{tia} (the displacement detection sensitivity in V/m). Since the goal of this particular experiment is to characterize specifically the displacement resolving characteristics of the approach, the system's sensitivity to ambient vibrations was removed by removing the proof mass from the system and replacing it with a rigid mirror. This removes external vibration noise from the measurement and allows the two dominant optical noise sources to be studied,

- Shot noise – the theoretical quantum noise limit which occurs at the photodiodes, and
- Laser intensity noise – small, broadband fluctuations in laser intensity

Since laser intensity noise occurs in both the zero and first diffracted orders, and since the signals are complementary, the common mode laser intensity noise can be cancelled without cancelling signal. This can be accomplished using a number of different approaches (Hobbs, 1997). An approach being investigated and developed by Silicon Audio was used to collect the data presented in Figure 8. With laser intensity noise cancellation, the displacement referred output noise is limited by shot noise, representing a displacement noise level of approximately 10fm/√Hz. This is lower than the resolution required for resolving the thermal mechanical noise of the proof mass and is a significant accomplishment of the Phase I study.

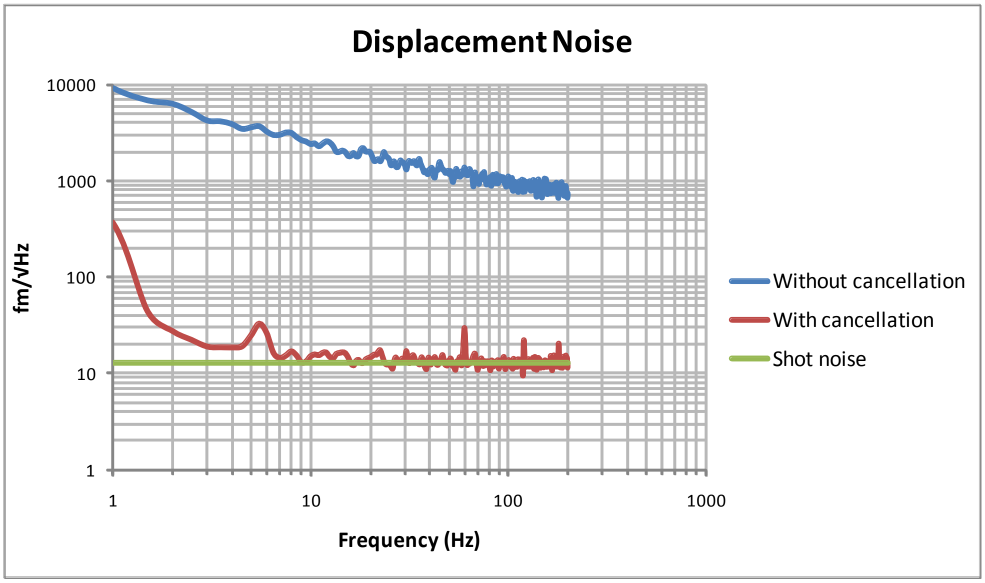

Figure 8. Measured displacement noise spectra of the Phase I prototype.

CONCLUSIONS AND RECOMMENDATIONS

Silicon Audio is addressing the NNSA's rigorous seismometer specifications using an approach that combines silicon micromachined optical elements, integrated semiconductor lasers, photodetection electronics, and meso-scale proof mass structures. This review article focused on a grating based implementation, and two significant Phase I accomplishments were discussed; high fidelity displacement detection and integration of feedback altered dynamics. Future development will focus on device design and noise mitigation for a 100-mHz–1-Hz frequency range, design for low cross axis sensitivity, and design for high thermal stability.

The timeliness of this innovative approach is worth noting. Low-cost, semiconductor lasers such as VCSELS are now fully commercialized and have been developed to the point where high quality, mode-stable, and polarization stable products are readily available. The movable grating actuator is readily fabricated with modern silicon microfabrication techniques. The vision for the Phase II development is a small, completely integrated, 3-axis sensor package roughly the size of a 9-volt battery.

ACKNOWLEDGEMENTS

The authors graciously thank the NNSA and the DOE SBIR program for support. We also thank the University of Texas, Institute of Geophysics for assistance with Phase I field test demonstrations.

REFERENCES

Hall, N. A. (2008). Micro-seismometers via advanced mesoscale fabrication, in *Proceedings of the Monitoring Research Review: Ground-Based Nuclear Explosion Monitoring Technologies*, LA-UR-08-05261, Vol. 1, pp. 610–614.

Hall, N. A., M. Okandan, R. Littrell, B. Bicen, and F. L. Degertekin (2007). Micromachined optical microphones with low thermal-mechanical noise levels, *J. Acous. Soc. Am.* 122 (4): 2031–2037.

Hall, N. A., M. Okandan, R. Littrell, D. K. Serkland, G. A. Keeler, and K. Peterson (2008). Micromachined accelerometers with optical interferometric read-out and integrated electrostatic actuation, *J. Microelectromech. Syst.* 17 :(1), 37–44.

Hobbs, P. C. D. (1997). Ultrasensitive laser measurements without tears, *Applied Optics* 36: (4): 903–920.

Lee, W., N. A. Hall, et al. (2004). Fabrication and characterization of a micromachined acoustic sensor with integrated optical readout. IEEE Journal on Selected Topics in Quantum Electronics 10: (3), 643–651.

Liu, C. H. and T. W. Kenny (2001). A high-precision, wide-bandwidth micromachined tunneling accelerometer, *J. Microelectromech. Syst.* 10: (3) 425–433.